Iraqi Journal of Industrial Research, Vol. 10, No. 1 (2023)

Open Access

Iraqi Journal of Industrial Research (IJOIR)

Journal homepage: http://ijoir.gov.iq

Mechanical and Physical Properties of Al_2O_3-TiAl deposited by Thermal Spraying Method

[1]Waleed A. Salih, [2]Salih Y. Darweesh*, [1]Sabah M. Aman Allah

[1]Department of Physics, College of Education of Pure Science, University of Kirkuk – Iraq

[2]Physics Department, College of Education, Tuz Khurmatu, Tikrit University – Iraq

Article information

Article history:
Received: March, 07, 2023
Accepted: April, 02, 2023
Available online: June, 14, 2023

Keywords:
Thermal spraying flame,
Vickers Hardness,
Stainless steel type 316L,
Ceramic

Corresponding Author:
Salih Y. Darweesh
salih.younis@tu.edu.iq

DOI:
https://doi.org/10.53523/ijoirVol10I1ID319

Abstract

In the current article, some physical properties of a system based on alumina (Al_2O_3) and supported by various weight ratios of TiAl were studied (5, 10, 15, 20, 25wt.%) by means of thermal spraying by flame, where oxygen gas was used at a pressure of 4bar, and acetylene at 0.7 bar. The base used for the coating is stainless steel type 316L, and a primary binder of 80%A1-20%Ni was coated with a thickness of approximately 100µm, while the base coating was 300µm thick, so that the total thickness was 400µm. The heat treatment of the final paint was carried out at a temperature of 1000°C for an hour and a half, after that physical tests were carried out through which the best mixing ratio was obtained, with a constant spraying distance of 16cm, and a constant spraying angle of 90° if found at that. The ideal conditions and after sintering that the best micro hardness is 56kg/mm^2, the least porosity is 9.1%, and the highest adhesion strength is 29, while the results of the scanning electron microscope showed that the best mixing ratio is the 25wt.% in which the surface was homogeneous and has a consistent composition. An indication of the improvement of the samples with the continuation of repeated additions of the support material (TiAl).

1. Introduction:

Thermal spraying is a general term used to define a group of processes for depositing metallic or non-metallic materials in a molten or semi-molten state on pre-prepared substrates for the purpose of painting [1]. Thermal spraying results in coatings with good properties that give the surface exposed to spraying high hardness and low wear rate [2, 3]. As for the materials that are sprayed, they are in the form of powder, rods, or metal wires [4]. Materials that are in a powder are heated, either by combustion of gases (such as flame spray) or Plasma Spray [5] The coating material turns into a plastic or molten state upon heating, and then is atomized and accelerated by compressing the gases. Which, in turn, transfers it to the base by forming a specific stream of droplets (the shape of the material during its transfer from the spray gun to the base). Lamellar structure [6, 7]. Flame spraying technology is the most common type of thermal spraying in the world because of its simplicity and low cost [8]. In this technique, the fuel gas combustion process is used with oxygen as a source of heat needed to melt the coating materials [9]. Hydrogen, propane and acetylene gases are used as gaseous fuels, and acetylene gas is one of the commonly used gases due to its low risk in work, in addition to its availability and low cost [10]. The flame

spraying technique generally gives coatings with acceptable properties though from the relatively low velocity of molten particles approximately 50 ms^{-1} and the low temperatures obtained from combustion. Flame approximately 3000℃ [11, 12]. Coating properties can be improved by processes called spray and fusion and Fuse Process, after the flame spraying process, the combustion process is used to raise the temperature of the base material to a degree close to the degree with which the paint material began to melt previously, and the result is a coating with a very high density and high adhesion. Because of the metallurgical bonding between the substrate and the coating layer [13, 14] .In the best conditions, when using an oxy-acetylene torch, it may reach 3100℃ [15, 16], which means limited using spray materials, the pressure of the combustion gases acts as a propellant for the particles and accelerates them to a speed of 100 ms^{-1} only [17]. The present article aims to study the variables of thermal spraying by flame, which included the mixing ratio on the physical properties for the resulting coating.

2. Raw Materials

Alumina was used as a base material produced by Central Drug House (CDH) of (Indian) origin, with a granular size of 100µm, and a purity of 99.7%. While the reinforcement material was made of Titania-Alumina (TiAl) metal, produced by (Metco 110), of (American) origin. With granular size (75µm) and purity (99.9%). As for the basic binding material, it is 80% A1-20%Ni produced by the company (Sulzer Metco) No. (443), of (Swedish) origin, with a granular size of 100µm and a purity of 99.9%.

3. Methodology

Sample preparation is essential to the success of a thermal spray coating... The degree of adhesion of the coating materials to the surface of the substrate depends on the mechanical interlocking of the solidified particles at the surface of the material basis. After the samples are cut and softened, they are washed with alcohol to remove fat or any other contaminants, taking into account not to holding it by hand throughout the preparation period, the grit blasting device manufactured by (Sabtux) was used. The Swedish granules are used to increase the surface roughness of the samples and the granules are silicon carbide or alumina granules with a range of diameters ranges from 0.7mm to 1.5mm. The prepared Cermet powder is sprinkled towards a base. coating using a spray gun type (GH-4/h) of Chinese origin, and the ratio of mixing oxygen with acetylene can be determined through a special regulator (Flowmeter), a special clamp is designed that holds the spray gun and installs it at different spray distances of (8, 12, 16, 20, 24) cm towards the sample bearing base. The best spraying parameters were selected by conducting a series of preliminary experiments to confirm to obtain coating layers with good adhesion strength and a certain thickness in order to qualify us to study the physical properties of this type of coating. The resulting samples of paint that were subjected to a thermal sintering process at 1000℃ for an hour and a half, after which it will be ready for physical examinations.

4. Examinations:

4.1. Scanning Electron Microscope (SEM)

The scanning electron microscope is one of the most important electronic microscopes in evaluating the topography of the surface, examining the surface structure and calculating the particle size, as well as it is possible to know the proportions of the constituent elements of the compound through (EDX), where a scanning electron microscope type (MIRA TESCAN) of Belgian origin was used. Through it, a beam of electrons is shed on the atoms present in the surface of the sample, and thus several different signals are produced that give information about the shape and topography of the outer surface of the samples used [18].

4.2. Porosity

Porosity is considered the preferred alternative for considerations of some packing characteristics of powders and it can be as the ratios of pores in powders to the bulk volume of the sample (Bulk Volume). The pores are of three types which are; closed pores, connected open pores, and separate open pores [19]. There are several factors that affect porosity, including the shape of the granules, their size and distribution, besides the strength of the bonding between the granules has a great effect on the porosity. An increase in fine granules relative to coarse granules means a decrease in porosity [20]. The pressure used for formation affects the proportion of pores [21]; because the use of high pressure will lead to an increase in compaction of granules and a decrease in porosity, the sintering temperature of the model for example, materials with low melting points within the composition will melt and fill the pores and reduce the porosity. The percentage of true porosity can be measured by the following relation [22]:

$$\mathbf{T.P.\%} = \frac{\mathbf{T.D.} - \mathbf{B.D.}}{\mathbf{T.D.}} \times \mathbf{100}\ \% \qquad (\mathbf{1})$$

Where: T.P: The total porosity ratio of the sample, B.D: The density of the sample in practice the density of the body (g/cm^3), T.D.: Theoretical sinter body density (g/cm^3).

4.3. Hardness

The hardness was tested using the Vickers method by inserting the tool (diamond pyramid four-base). By shedding the tool with a mass of 500 g for a period of (10), and by calculating the diameters of the resulting trace, the Vickers hardness of the pressed object can be known through the application of Equation (2), a French Vickers Hardness measuring device was used. As 10 readings were recorded for one press, 5 readings for each face of the press (in a radial manner from the center of the surface of the press to its periphery, then the average of these readings was calculated. The results of the readings were very close, indicating the homogeneity of the surface and the absence of almost any internal defects, the relationship Vickers hardness value [23].

$$\mathbf{HV} = \frac{2F\ Sin\ 136°/2}{d} \approx \mathbf{1.854\ F/d^2} \qquad \mathbf{(2)}$$

It represents: F: The amount of load imposed in Newton, d: the average impact diameter in mm.

4.4. Adhesion Strength

The adhesion measurement of the coating layer was carried out using a tensile device with a maximum load of 2 tons according to the standard specification (ASTM - (C633) [24]. Preparing samples of the base material without coating with an equal number of sprayed and non-sprayed samples Chemical cleaning operations were carried out by using alcohol to clean all samples in order to get rid of fat, dust and any other contaminants that hinder the process of gluing the two pieces together, after that an epoxy adhesive was used to stick the two pieces together (sprayed and not sprayed).A thin layer of adhesive was placed on the surface of the paint so that it covered all parts of the surface, taking into account that it was regular. Then the two pieces were pressed together for a period of 1hr and then placed in a drying oven for a period of (24 hours) at a temperature of 50℃. Before conducting the tensile test, the adhesion must be regular and the tensile force applied when conducting the test should be perpendicular to the surface of the coating. After the sample is installed in the tensioning device, a tensile load is applied to each test sample at a tensile rate (1 mm/min) until the sample fails where the highest projected load is recorded .

5. Results and Discussion

5.1. Effect of Hardener on the Vickers Hardness of Cermet Coating

Figure (1) shows the relationship between the stiffening material (TiAl wt.%) and the micro-Vickers hardness before and after the thermal sintering process at a temperature of 1000℃ for a 1.5 hour. (TilA) at 5wt.% is 27 kg/mm^2 before sintering and 34 kg/mm^2 after sintering, while the hardness value at 25wt.%TiAl was 46 kg/mm^2 before sintering and 56 kg/mm^2 after sintering, Thus, find that the hardness value has increased after thermal sintering than before, and this is due to the influence of the reinforcing material (50%Ti-50%A1), which is characterized by high hardness and almost excellent bonding strength, which contributed effectively to diffusion through the base material (Al_2O_3), where the minerals are distinguished on diffusion through the oxides, thus forming an alloy with high durability and excellent mechanical interlocking [25], as well as the thermal sintering process has an effective effect on bridging the voids and distances between the two materials base besides the reinforcement. The convergence of the atoms from each other, which helps the bonding between the metal and the ceramic as the temperature (1000℃) for an hour and a half contributed to this lattice fusion and obtain high hardness the obtained high hardness values. As a result of the use of powders with a grain size ranging from 75-100 µm, it is related to the grain size. The smaller the granule sizes, the more they provide greater obstruction areas for the plastic deformations resulting from the penetration of the sticking tool to test the hardness, on the contrary, if the granule sizes are large, they will have fewer disabilities and thus plastic deformities will be greater [26, 27].

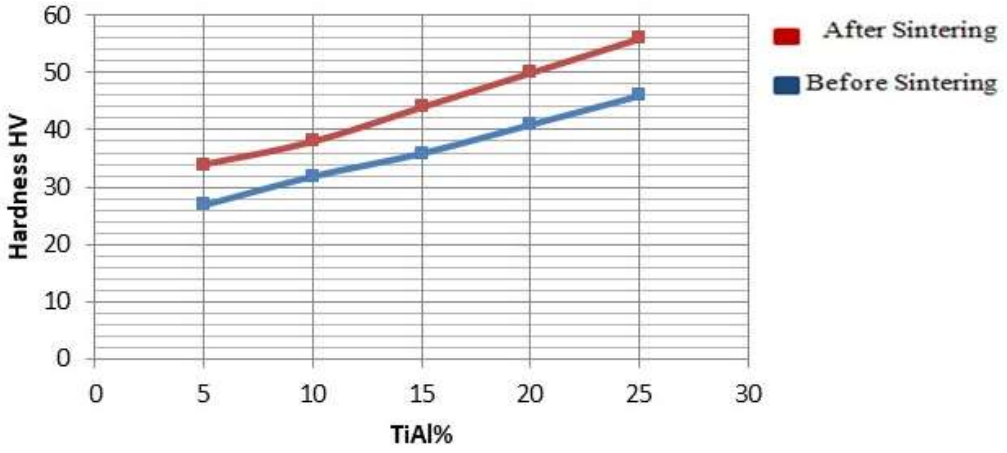

Figure (1). The Vickers hardness with the reinforcement material before and after the thermal sintering process.

5.2. Effect of Stiffener on the Porosity of the Cermet Coating

Figure (2) show the relationship between the reinforcing material (TiAl wt.%) and its porosity before and after the thermal sintering process at a temperature of 1000℃ for 1.5 hour. The result that the porosity decreasing with the increasing of the reinforcing material, so the value of the porosity was at 5wt.%TiAl is 25.5% before sintering and 20.2% after sintering. The highest percentage of porosity was observed before sintering (25.5%) and is attributed to the surface roughness and to the increase in gas pressure confined in the closed pores, which allow cracks to form, which in turn work on raising the values of porosity, while the value of porosity at 25wt.% TiAl was 11.5% before sintering, and the value of porosity was 9.11% after sintering. Where it is noted that the values of porosity began to decline when the sintering procedure and the temperature (1000℃), at which the rate of diffusion of atoms is sufficient to form good bonding areas between the layers, thus trying to close the pores [28, 29].

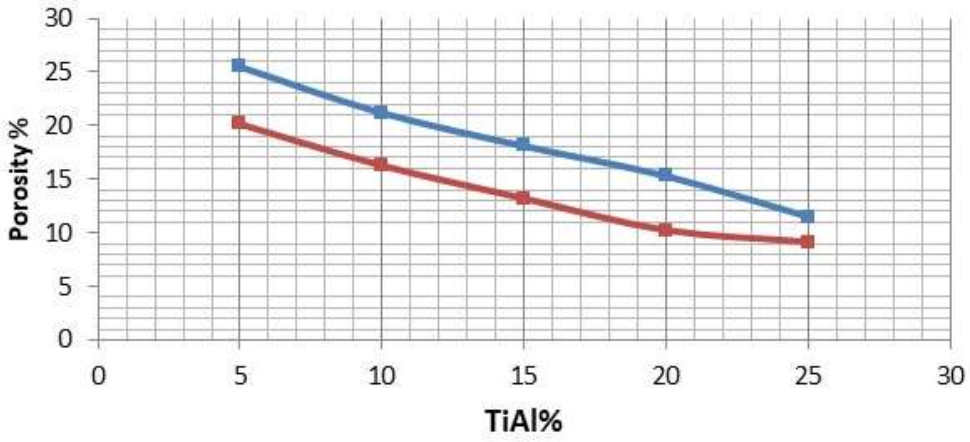

Figure (2). The porosity with the support material before and after the sintering process.

5.3. Effect of Stiffener on Adhesion Strength of Cermet Coating

Figure (3) shows the relationship between the reinforcing material (TiAlwt.%) and the adhesion strength before and after the thermal sintering process at a temperature of (1000℃) for a 1.5hour. This figure indicates that the adhesion strength increases with the increase of the reinforcing material that the adhesion strength increases with the increase in the reinforcing material, so the value of the adhesion strength was for 5%wt.TiAl it is 8MPa before sintering and 11MPa after sintering, while the value of adhesion strength at 25wt.%TiAl was 22 MPa before sintering, and it was 29 MPa after sintering, adhesion strength can be defined as the force equivalent to the force needed to remove a unit area of the coating layer from the cermet base If the sintering process clearly contributes to increasing the adhesion strength, as the sintering process leads to an increase in the kinetic energy of the material, and thus the vibrations of the coating particles increase, which makes the atoms of the coating material approach each other and thus they are more sticky and cohesive [30, 31].

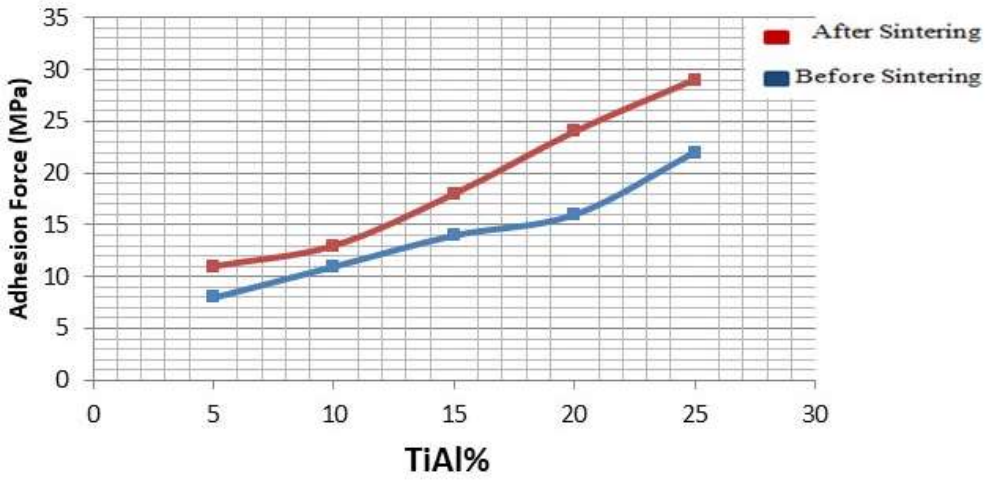

Figure (3). The adhesion strength with the support material before and after the thermal sintering process.

5.4. Scanning Electron Microscope (SEM) Test

Through the scanning electron microscope (SEM) images, shown in Figure (4) the composite (Al_2O_3-TiAl) at a depth of 5µm, with a magnification of 10kx, after conducting thermal sintering for all samples and in ideal conditions with a fixed (angle Spraying 90°, a spraying distance of 16 cm). In Figure (4-a) with a reinforcement percentage of 5wt.% TiAl after the heat treatment (sintering), we notice that the is homogeneous, but somewhat random, but the effect of heat is clear through the adhesion of the granules to each other with the spread of some surface defects somewhat with the pores in the microstructure [32]. It is also noted that there are areas of low density and others of high density, which led to the spacing of the elements from each other and their heterogeneity. As for Figure (4-b), at a ratio of 10wt.%TiAl, the microstructure appears more homogeneous with stronger and greater bonding as a result of fusion of titanium and aluminum with alumina components compared to model (a), and that there is an overlap between the particles of both powders, as well as a clear presence of some. The visible pores through the surface of the sample [33].

As for the Figure (4-c), at the reinforcement percentage (15wt.% TiAl), we notice a large distribution of the reinforcement material, this is evident through the spread of clear granules on the surface and coalesced with each other forming a metal network with the presence of few pores that permeate it. As for Figure (4-d), with an increase in the reinforcement ratio to 20wt.% TiAl, as a result, there is an increase in the adhesion ratio between the alumina granules and the reinforcement granules an increase in the adhesion ratio between the alumina granules and the granules of the reinforcement material, with the beginning of an improvement in the microstructure and the process of filling the pores by aluminum. As for Figure (4-e), where the percentage of support is at 25wt.% TiAl. Thus a large ratio of titanium – aluminum has a clear effect on the distribution and complete melting of aluminum between the alumina compounds, with a clear disappearance of the pores and the lack of surface defects, i.e. recrystallization of the supported bonding granules, which means the formation of a layer with a strong structural structure, which can be used in many engineering and industrial applications that require high surface strength and durability [34].

The examining by X-ray spectroscopy (EDX), of the materials used during the work, as shown in Figure (4), where find the appearance of the base material (Al_2O_3) and the two support materials (Al), (Ti) and also find the separation of oxygen from aluminum due to heat. We also find the appearance of nickel, which is the binder in the first coating layer.

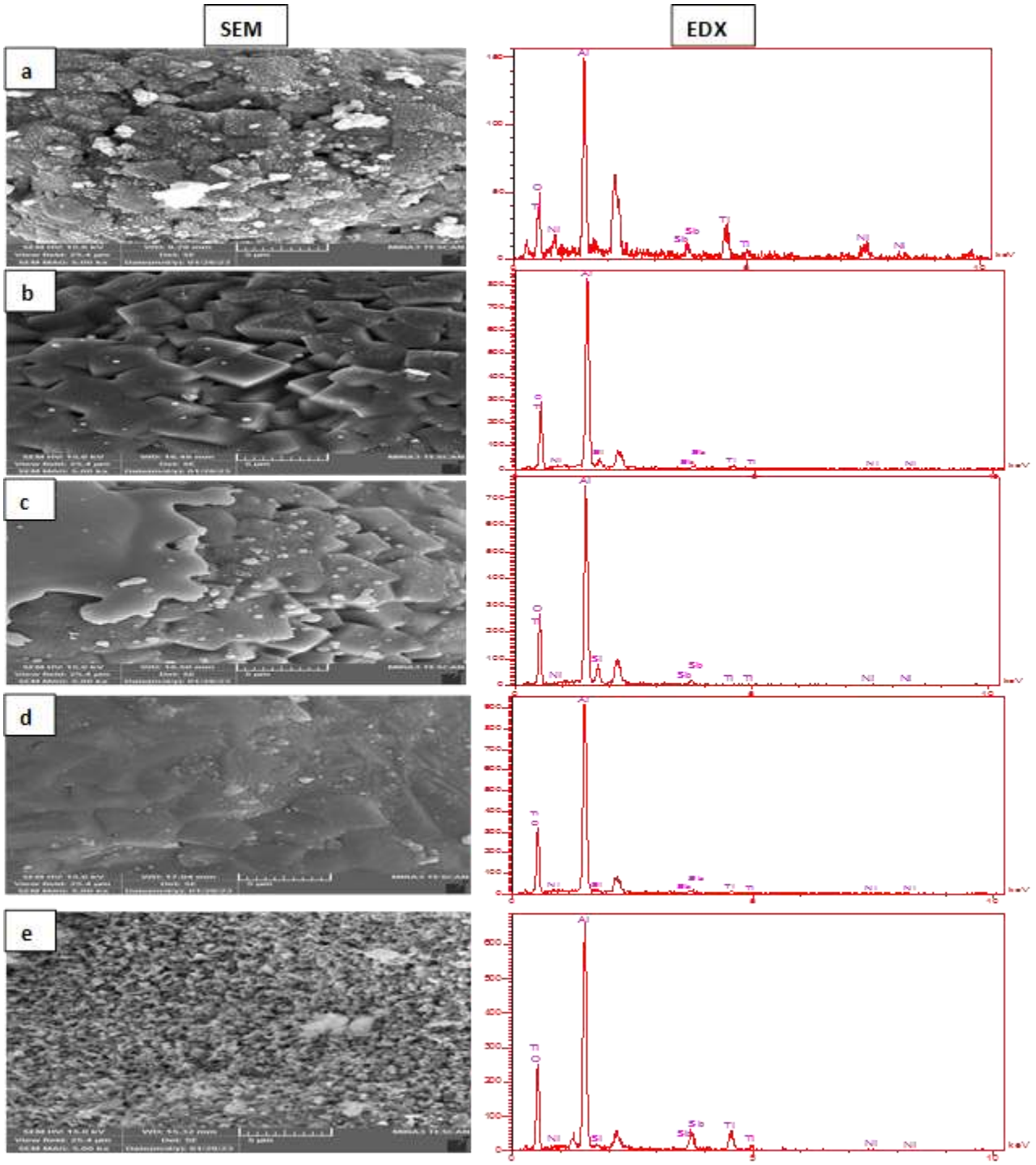

Figure (4). Scanning Electron Microscope images at different support concentrations: (a = 5%, b = 10%, c = 15%, d = 20%, e = 25%) after thermal sintering.

6. Conclusions

The important conclusion from the current article is the possibility of strengthening an oxide material such as alumina with a metal material, which is TiAl in different weight ratios of the reinforcement material. It was found that the best mixing ratio is 25wt.%, and then it was found that the hardness value is 56kg/mm^2, the porosity is 9.1% and the adhesion strength is 29MPa after thermal sintering, while the results of the scanning electron microscope gave an almost distinct surface shape at 25wt.%. An indication of the improvement of the crystal structure with each increase of the reinforcing material.

References

[1] F. Meierhofer, U. Fritsching "Synthesis of metal oxide nanoparticles in flame sprays: review on process technology, modeling, and diagnostics", *Energy & Fuels*, vol. 35, no. 7, pp. 5495-5537, 2021.

[2] M. Dorfman, "Thermal spray coatings", In Handbook of environmental degradation of materials, William Andrew Publishing, pp. 469-488, 2018.

[3] P. Fauchais, A. Vardelle, "Thermal sprayed coatings used against corrosion and corrosive wear", *Advanced plasma spray applications*, vol. 10, pp. 34448, 2012.

[4] P. Fauchais, J. Heberlein, M. I. Boulos, "Thermal spray fundamentals: from powder to part", *Springer Science & Business Media*, 2014.

[5] R. Gonzalez, H. Ashrafizadeh, A. Lopera, P. Mertiny, A. Mcdonald, A review of thermal spray metallization of polymer-based structures. Journal of Thermal Spray Technology, vol. 25, 897-919. (2016).

[6] A. Nouri, A. Sola, "Powder morphology in thermal spraying",*Journal of Advanced Manufacturing and Processing*, vol. 1, no. 3, pp. e10020, 2019.

[7] V. Boronenkov, Y. Korobov, "Fundamentals of arc spraying". *Physical and Chemical Regularities; Springer: Berlin/Heidelberg*, Germany, 2016.

[8] A. Vardelle, C. Moreau, N. Themelis, C. Chazelas, "A perspective on plasma spray technology", *Plasma Chemistry and Plasma Processing*, vol. 35, pp. 491-509, 2015.

[9] K. Sunitha, H. Vasudev, "A short note on the various thermal spray coating processes and effect of post-treatment on Ni-based coatings", *Materials Today: Proceedings*, vol. 50, pp. 1452-1457, 2022.

[10] S. Kahar, A. Singh, U. Vala, A. Desai, S. Smit Desai, "Thermal sprayed coating using zinc: A review", *IRJET*, vol. 7, no. 6, pp. 6497-6503, 2020.

[11] T. Liao, A. Biesiekierski, C. Berndt, P. King, E. Ivanova, H. Thissen, P. Kingshott, "Multifunctional cold spray coatings for biological and biomedical applications: A review", *Progress in Surface Science*, vol. 100654, 2022.

[12] M. Sauter, A. Roth, A. Grebhardt, A. Killinger, "High velocity flame spraying of highly-filled ceramic-Polymer filaments (F-HVOF)", *Surface and Coatings Technology*, vol. 129324, 2023.

[13] L. Berger, "Application of hardmetals as thermal spray coatings", *International Journal of Refractory Metals and Hard Materials*, vol. 49, pp. 350-364, 2015.

[14] E. Sadeghi, N. Markocsan, S. Joshi, "Advances in corrosion-resistant thermal spray coatings for renewable energy power plants. Part I: Effect of composition and microstructure", *Journal of Thermal Spray Technology*, vol. 28, pp. 1749-1788, 2019.

[15] A. Vardelle , C. Moreau, J. Akedo, H. Ashrafizadeh, C. Berndt, J. Berghaus, P. Vuoristo, "The thermal spray roadmap", *Journal of thermal spray technology*, vol. 25, pp. 1376-1440. 2016.

[16] A. Lynam, A. Romero, F. Xu, R. Wellman, T. Hussain, "Thermal spraying of ultra-high temperature ceramics: A review on processing routes and performance", *Journal of Thermal Spray Technology*, vol. 31, no. 4, pp. 745-779, 2022.

[17] X. Yang, W. Shang, H. Lu, Y. Liu, L. Yang, R. Tan, Y. Shen, "An agglutinate magnetic spray transforms inanimate objects into millirobots for biomedical applications", *Science robotics*, vol. 5, no. 48, pp. eabc8191, 2020.

[18] C. Prasad, S. Joladarashi, M. Ramesh, "Comparative investigation of HVOF and flame sprayed CoMoCrSi coating", *In AIP Conference Proceedings*, AIP Publishing LLC, vol. 2247, pp. 050004, 2020.

[19] W. Wong, P. Vo, E. Irissou, A. Ryabinin, J. Legoux, S. Yue, "Effect of particle morphology and size distribution on cold-sprayed pure titanium coatings", *Journal of thermal spray technology*, vol. 22, pp. 1140-1153, 2013.

[20] M. Azizpour, M. Tolouei-Rad, "The effect of spraying temperature on the corrosion and wear behavior of HVOF thermal sprayed WC-Co coatings", *Ceramics International*, vol. 45, no. 11, pp. 13934-13941, 2019.

[21] P. Khamsepour, J. Oberste-Berghaus, M. Aghasibeig, F. Ettouil, A. Dolatabadi, C. Moreau, "The Effect of Spraying Parameters of the Inner-Diameter High-Velocity Air–Fuel (ID-HVAF) Torch on Characteristics of Ti-6Al-4V In-Flight Particles and Coatings Formed at Short Spraying Distances",*Journal of Thermal Spray Technology*, pp.1-18, 2023.

[22] E. Salih, S. Allah, S. Darweesh, H. Mohammed, " Study of some of the physical variables of a metal-based system using the powder method", *In Journal of Physics: Conference Series*, IOP Publishing, vol. 1999, pp. 012068, 2021.

[23] R. Tan, "Development of Alumina Based Feedstock for Fused Deposition Modelling 3D Printer", Doctoral dissertation, UTAR, 2020.
[24] T. Mishra, A. Kumar, S. Sinha, "Experimental investigation and study of HVOF sprayed WC-12Co, WC-10Co-4Cr and Cr3C2-25NiCr coating on its sliding wear behavior", *International Journal of Refractory Metals and Hard Materials*, vol. 94, pp. 105404, 2021.
[25] D. Kim, S. Cho, J. Choi, J. Koo, C. Seok, M. Kim, "Evaluation of the degradation of plasma sprayed thermal barrier coatings using nano-indentation", *Journal of Nanoscience and Nanotechnology*, vol. 9, no. 12, pp. 7271-7277, 2009.
[26] X. Wang, Y. Zhou, "Layered machinable and electrically conductive Ti2AlC and Ti3AlC2 ceramics: a review", *Journal of Materials Science & Technology*, vol. 26, no. 5, pp. 385-416, 2010.
[27] I. Gibson, D. Rosen, B. Stucker, M. Khorasani, D. Rosen, B. Stucker, "Additive manufacturing technologies", Cham, Switzerland: Springer, vol. 17, 2021.
[28] F. Cernuschi, L. Lorenzoni, S. Ahmaniemi, P. Vuoristo, T. Mäntylä, "Studies of the sintering kinetics of thick thermal barrier coatings by thermal diffusivity measurements", *Journal of the European Ceramic Society*, vol. 25, no. 4, pp. 393-400, 2005.
[29] Y. Wu, D. He, "High-temperature sintering resistance of novel NdYbZr2O7 thermal barrier coating", *Surface and Coatings Technology*, vol. 129275, 2023.
[30] F. Xu, H. Yao, K. Tang, Y. Li, F. Han. Z. Tan, Z. Zhou, "Degeneration of thermal insulation property for Fe-based amorphous coating during long-term heat exposure", *Journal of Non-Crystalline Solids*, vol. 606, pp.122203, 2023.
[31] S. Darweesh, A. Ali, Z. Khodair, Z. Majeed, "The effect of some physical and mechanical properties of cermet coating on petroleum pipes prepared by thermal spray method", *Journal of Failure Analysis and Prevention*, vol. 19, pp. 1726-1738, 2019.
[32] S. Mohammed, S. Darweesh, "Effect of thermal treatment on some physical and mechanical properties of cermet coating by flame spraying technology",*Journal of University of Babylon for Pure and Applied Sciences*, vol. 26, no. 7, pp. 269-280, 2018.
[33] H. Ahmed, A. Ahmed, S. Darweesh, Z. Khodair, M. Al-Jubbori, "Processing of Turbine Blades Using Cermet Composite Materials", *Journal of Failure Analysis and Prevention*, vol. 20, pp. 2111-2118, 2020.
[34] A. Jassim, S. Darweesh, S. Humeedi, "Using thermal spray coating method to produce system composites (Ni-Al2O3-B4C", *Tikrit Journal of Pure Science*, vol. 27, no. 5, pp. 68-75, 2022.
[35] F. Pedraza, M. Mollard, B. Rannou, J. Balmain, B. Bouchaud, G. Bonnet, "Potential thermal barrier coating systems from Al microparticles. Mechanisms of coating formation on pure nickel", *Materials Chemistry and Physics*, vol. 134, no. 2-3, pp. 700-705, 2012.